

Formation of zirconium dioxide layers on microelectrode of zirconium. Inhibition of the hydrogen evolution reaction

L. Pospíšil^{1*}, N. Fanelli², M. Hromadová¹

¹ J. Heyrovský Institute of Physical Chemistry, CAS v.v.i., Dolejškova 3, Prague, Czech Rep.

² Institute of Chemistry of Organometallic Compounds, CNR Pisa, via Moruzzi 1, Pisa, Italy

Received September 30, 2016 Revised October 29, 2016

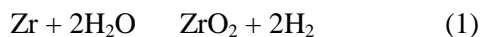
Electron transfer reactions on high purity grade Zr microelectrode were investigated in borate buffer. Oxidation producing a surface layer of ZrO₂ occurs at potentials more positive than -0.5 V (against Ag|AgCl|1M-LiCl). Surface layer effectively retards the hydrogen evolution reaction. Mechanistic information was obtained by the application of cyclic voltammetry and electrochemical impedance spectroscopy.

Key words: zirconium, ZrO₂, corrosion, impedance, hydrogen evolution.

INTRODUCTION

Pioneering work of professor Zdravko Stoynev was devoted to the development of innovative methods of electrochemical impedance analysis for various aspects of the power sources development [1]. Our contribution to a special issue celebrating his anniversary deals with impedance characteristics of zirconium used in the nuclear power plants.

Zirconium and its alloys are materials essential for the nuclear power plants, where they find use as cladding of the active fuel. The choice of Zr is due to its very low thermal neutron-capture cross-section, high hardness and resistance to corrosion. Nuclear-grade zirconium alloys contain about 95 % of zirconium and less than 2% of tin, niobium, iron, chromium, nickel and other metals, which are added to improve its mechanical properties. One disadvantage of zirconium alloys is that zirconium reacts with water at high temperatures, producing hydrogen gas and accelerated degradation.



Oxidative reaction of zirconium with water releases hydrogen gas, which partly diffuses into the alloy and forms zirconium hydrides. The hydrides are less dense and are weaker mechanically than the alloy. Formation of hydrides leads to blistering and cracking which is called hydrogen embrittlement. The redox reaction is causing the instability of fuel supports at high temperatures though it is slow at low temperatures. This reaction was responsible for a small hydrogen

explosion at the Three Mile Island nuclear power plant and in Fukushima I nuclear power plant disaster initiated by the earthquake. Hence the mechanism of the hydrogen evolution reaction (HER) on zirconium and zirconium dioxide layers is an issue.

Oxidation of zirconium occurs at the same rate in air or in water and proceeds in the ambient condition or in high vacuum. The rate of oxidation was measured at various temperatures and pressures [2]. A sub-micrometer thin layer of zirconium dioxide is rapidly formed at the surface and stops further diffusion of oxygen to the bulk and the subsequent oxidation. ZrO₂ adopts a monoclinic crystal structure at room temperature, which transforms to tetragonal and cubic at higher temperatures. The volume expansion caused by the cubic to tetragonal to monoclinic transformation induces large stresses upon cooling, and these stresses cause ZrO₂ to crack. The oxide layer is a semiconductor. The ZrO₂ band gap is dependent on the phase (cubic, tetragonal, monoclinic, or amorphous) and preparation methods, with typical estimates from 5–7 eV [3]. Numerous studies were devoted to Zr corrosion [4]; nevertheless operating conditions require a continuous improvement of protection techniques. Electrochemical impedance was investigated under high temperature and the open circuit potential with the aim to identify the layer thickness [5, 6]. Conditions were selected to those of various types of nuclear reactors [7-9].

This communication summarizes our results aimed at characterization of possibly oxide free Zr surface and the kinetics of growth of ZrO₂ layer at early stages of its formation. In difference to experiments at the open circuit potential and operating conditions we explored the characteristics of HER at controlled applied potential and at

To whom all correspondence should be sent:
E-mail: pospasil@jh-inst.cas.cz

ambient conditions using zirconium without the presence of additional metals.

EXPERIMENTAL

Zirconium wire of 0.25 mm diameter was purchased from Alfa Aesar of 99.95% purity grade containing metallic impurity of 29 ppm Hf, 190 ppm Fe, 1.8 ppm Cu, 8.4 ppm Cr and 4.1 ppm Ni. Wire was soldered to a support copper wire, inserted in a thick walled tight glass capillary and fixed with a TorrSeal™ resin. The exposed part of the wire was polished with the emery paper Schmirgelpapier 6/0 (SIA, Switzerland). Only the small polished disc was in contact with the solution. This served as the working electrode. The auxiliary electrode was a Pt wire of approximately 100-times larger area compared to Zr electrode. The reference electrode was Ag|AgCl|1M-LiCl electrode separated from the sample by a salt bridge. Borate buffer pH 8.25 contained 0.2 M boric acid and 0.05 M sodium tetraborate. Sample was degassed by a stream of argon. Electrochemical measurements were made using potentiostat/galvanostat PGSTAT30 with frequency analyzer option (Metrohm, Switzerland). Data were analyzed by means of ZView software, version 3.2b (Scribner Associate, Inc., North Carolina, USA).

RESULTS AND DISCUSSION

Cyclic voltammetry was used for identification of the potential ranges, where the zirconium surface remains relatively free of oxide and where the ZrO_2 layer is formed. The initial and vortex potentials of experiments were optimized together with the surface treatment. We found that only dry polishing leads to reproducible voltammograms. Wet polishing with alumina slurry or contact of a polished surface with rinsing water immediately produced certain oxide formation.

Figure 1 shows subsequent voltage scans without polishing between scans. Anodic waves at -0.2, +0.7 and +1.2 V correspond to the oxidation of Zr to its dioxide. Each subsequent scan displaces the wave toward more positive potentials. The shift indicates that the originally formed layer may still contain vacancies, which can be filled with ZrO_2 . The cathodic current at the most negative potentials (< -1.0V) corresponds to the hydrogen evolution reaction. Evidently, the oxide layer of different compactness inhibits the hydrogen reaction to a different extent. When the polished electrode was inserted into the solution with an immediate potential control at -0.7 V the oxidation wave occurred at -0.5 V. Repeated polishing and the resulting limited reproducibility is shown in Figure

2. For the rest of our experiments we used this procedure. Anodic oxidation yields a wave-shaped curve instead of typical voltammetric peak-shaped current-voltage dependence. This signifies that the mass transport is absent and the redox step indeed involves metallic zirconium.

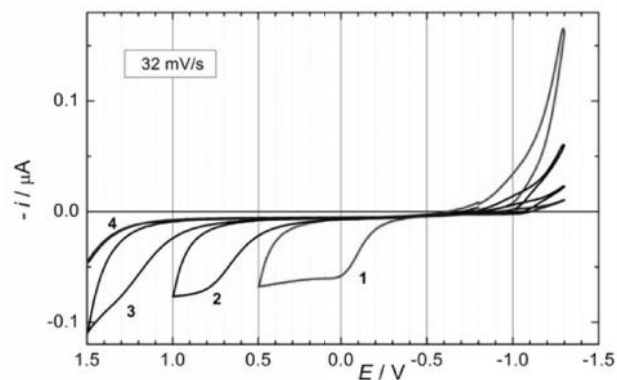


Fig. 1. Cyclic voltammogram of Zr disc of 250 μm diameter fitted in glass. Solution was the borate buffer 0.2 M boric acid and 0.05 M sodium tetraborate. The scan rate was 32 mV/s initiated at -0.7 V toward positive potentials. Three subsequent scanning cycles without polishing the surface: 1st cycle (red), 2nd and 3rd cycles in black. The blue curve corresponds to a covered surface.

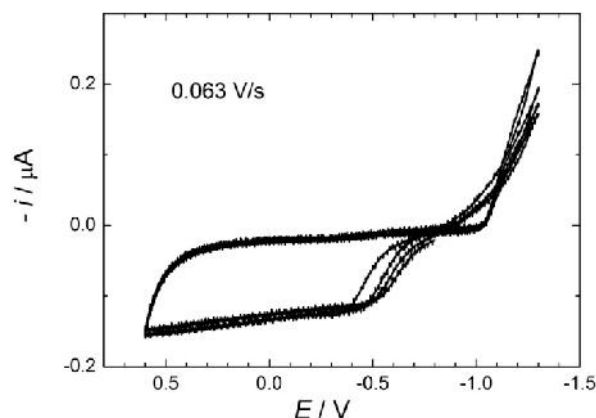


Fig. 2. Cyclic voltammogram of Zr in the same solution as in Figure 1. The surface was polished by the emery paper prior to each scan. The contact of the electrode with the solution was made under application of -0.8 V.

The dependence of the anodic wave height on the voltage scan rate from 0.032 V/s to 1 V/s is linear confirming thus a surface-bound redox reaction.

Further characterization was performed by application of AC techniques, firstly by the phase sensitive AC voltammetry (Figure 3). Scanning the freshly polished electrode from negative to positive potentials causes a gradual decrease of the imaginary admittance component Y'' , which is proportional to the double layer capacitance C . At positive potentials $Y'' \sim C$ is about one half of the original value. The second scan yields only a low value of Y'' . Observed picture confirms an

irreversible formation of a surface layer. AC voltammetry does not yield a detectable faradaic maximum at 160 Hz of the superimposed sine voltage. However, by lowering the frequency of the applied signal to 16 Hz, one can distinguish a peak on the real admittance component located at potentials, where the cyclic voltammograms show the anodic wave (Fig. 4).

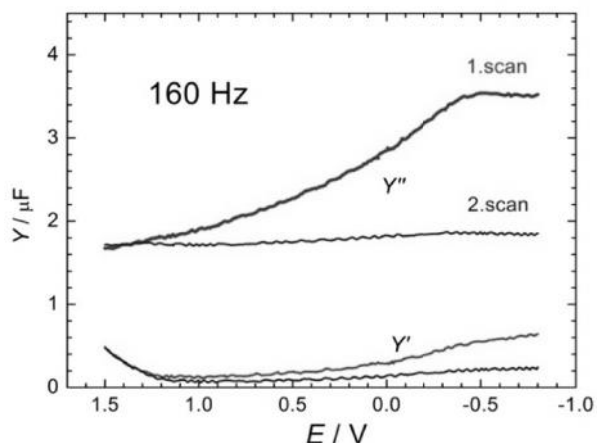


Fig. 3. The phase-sensitive AC voltammetry of Zr microelectrode in the same solution as in Figure 1. Upper curves are the imaginary admittance components, the lower curves correspond to the real admittance vector component. Curve labels distinguish the first and the second subsequent scan. The initial potential was -0.8 V and the DC applied voltage was scanned at 10 mV/s.

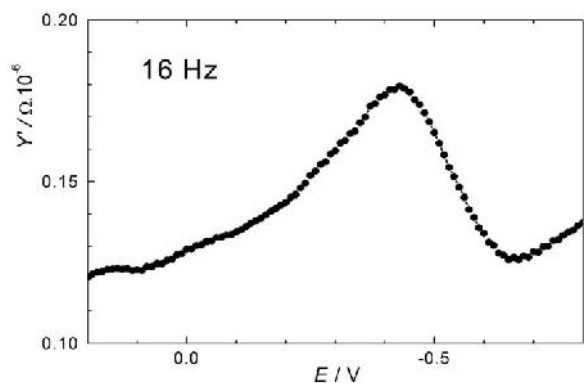


Fig. 4. The real admittance vector component of the phase-sensitive AC voltammetry of Zr microelectrode in the same solution as in Figure 3. The applied frequency was 16 Hz and the amplitude was 10 mV. The initial DC potential was -0.8 V and the DC applied voltage was scanned at 10 mV/s. The imaginary component showed no faradaic maximum.

Since there was no faradaic maximum at the imaginary admittance component, we can conclude that the electron transfer producing the oxide layer is very slow. We examined the time dependence of the double layer capacitance, which yields an estimate of conditions to get a final complete oxide layer.

A potentiostatic step pulse was applied, after which the Y'' values were recorded (Figure 5). For

the step to $+0.3$ V the final low double layer capacitance value is not reached even after 300 sec, whereas a step to $+0.6$ V produced a stable layer within less than a second. Information collected from these experiments was used for exploration of the hydrogen evolution reaction (HER).

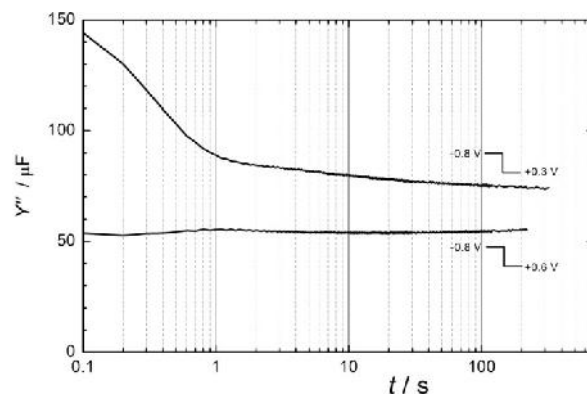


Fig. 5. The time dependence of the imaginary admittance component of Zr electrode in borate buffer measured at 160 Hz. The DC potential was stepped as indicated for respective curves.

Firstly, we applied electrochemical impedance spectroscopy (EIS) for control of the polishing quality. Irreversible electron transfer like HER, is very sensitive to the surface coverage. Hence, the lower the charge transfer resistance the less oxide is on the zirconium surface. The electrode, which was dry polished, was immediately inserted in the cell against a stream of argon. Electrical connections have been already made and hence the electrode was polarized to -0.8 V upon contact with the solution. The electrode potential was stepped to -1.50 V and the EIS data were collected. Figure 6 shows three successive polishing (full points) leading to a minimum R_{ct} and two EIS spectra of deliberately oxidized surface at 0.00 V (hollow points).

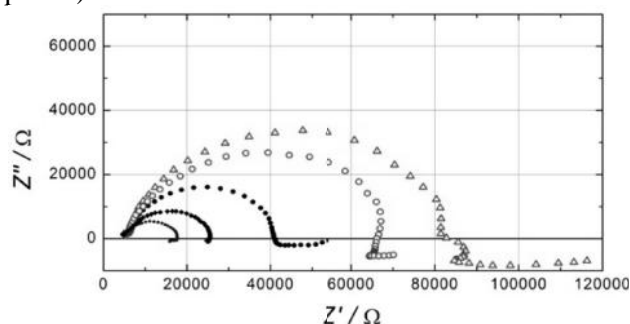


Fig. 6. The complex impedance plot of Zr electrode in borate buffer and polarized to -1.50 V. Three curves plotted with full points show subsequent polishing leading to the lowest observed value $R_{ct} = 12.4$ k Ω . Two large semicircles (hollow points) correspond to the deliberately oxidized surface kept at 0 V for 30 and 60 seconds.

Partial oxidation of Zr surface causes also low frequency loops with negative imaginary impedance. Data at the lowest frequencies are not suitable for interpretation because they are influenced by time changes of the surface during EIS measurements. This was confirmed by the application of the Kramers–Kronig relations, which often failed to confirm causality below 1 Hz. Low frequency loops are better developed at less negative potentials.

Performing EIS at different potentials using meticulously polished Zr electrode yields the dependence of the charge transfer resistance of hydrogen evolution on the applied potential (Figure 7). Measurements were repeated at each potential and only data with the lowest circle diameter of the Nyquist plot were accepted. Values of R_{ct} were obtained by two methods, fitting data to a circle and fitting to an equivalent circuit of ladder type (Chart 1).

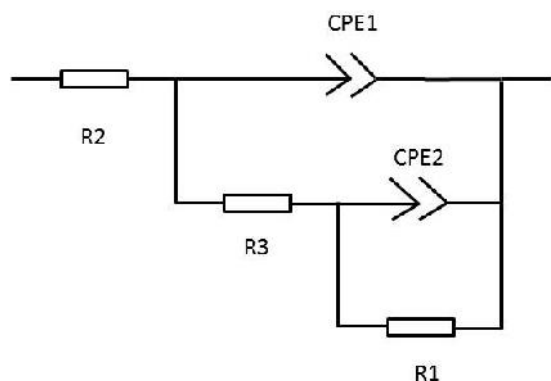


Chart 1. Ladder type equivalent circuit used to estimate R_{ct} and CPE1 by Z-view software.

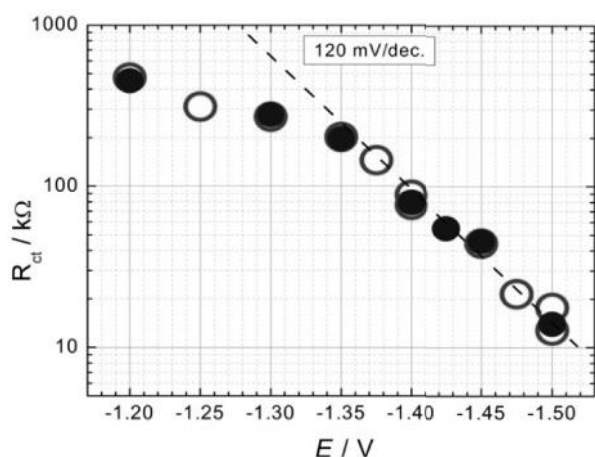


Fig. 7. The dependence of the charge transfer resistance of HER on polished Zr in borate buffer. Data fitting to a circle are hollow points. Fitting to a ladder circuit is shown as filled points.

The dependence R_{ct} vs E yields an asymptote with the slope of 120 mV/decade, which corresponds to the one-electron irreversible reduction and the transfer coefficient $\alpha = 0.5$. The CPE1 element at different potentials is shown in

Figure 8. Decreasing values toward less negative potentials may reflect accentuated adsorption effects.

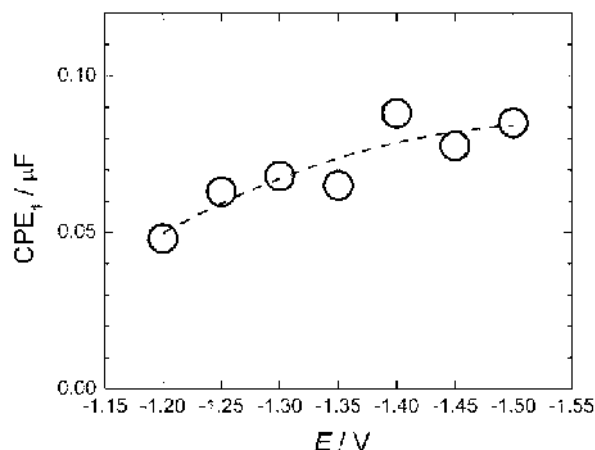


Fig. 8. The dependence of the constant phase element CPE1 on the applied potential. Data were obtained by the same fitting as those given in Figure 7.

Small low frequency loops, which were already noticeable on polished electrode at -1.5 V (see Figure 6) become quite large when the Zr surface is oxidized. Appearance of two large circles in EIS spectra of oxidized electrodes led us to use the ladder circuit for data analysis. An example is given in Figure 9 and the corresponding data in Table 1.

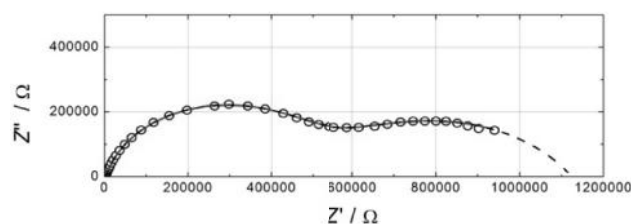


Fig. 9. The complex impedance plot of Zr electrode in borate buffer. The surface was oxidized for 60 seconds at the potential +0.5 V and data were measured at -1.20 V. Data are shown as circles, the solid line shows fitted data and the dashed line represents the simulation to 1 MHz using fitted parameters.

Table 1. Results of fitting EIS data in Figure 9 using the ladder circuit given in Chart 1

Element	Value	Error %
R2	3761	0.12
R3	533930	0.033
R1	586610	0.074
CPE1-T	15.1 nF	0.10
CPE1-P	0.85	0.018
CPE2-T	1.05 μF	0.047
CPE2-P	0.62	0.06

The reproducibility of the second CPE2 element and the corresponding R1 resistance were not sufficient for suggesting a quantitative interpretation.

The low frequency loops with positive or negative elements indicate the electron transfer coupled with the adsorption of one or two species [10]. Adsorption of hydrogen in metals and alloys is of importance in the field of fuel cells. Therefore a large amount of reports is focused on this phenomenon. The direct (one-step) insertion reaction mechanism was introduced by Bagotskaya and Frumkin [11]. Indirect (two-step) insertion of hydrogen in metals and alloys was thoroughly treated in several studies of Montella's group [12]. Nyquist plots presented here qualitatively resemble systems, where HER proceeds in the presence of a deposited surface layer (see for example report of Castro et al. [13]). EIS for those cases was analyzed using the equivalent circuit related to the HER according to the Volmer-Heyrovský-Tafel mechanism. The model used here (Chart 1) follows the same line. The properties of low frequency loop(s) are determined by rather complicated combination of adsorption and kinetic parameters reflecting the influence of the coverage of redox active species on the electron transfer rate and vice versa [10]. The present case is still more complicated because the adsorption of hydrogen may involve Zr and/or ZrO₂ surfaces. Indeed the negative loops in Figure 6 can be simulated (Figure 10) though the data fitting is still not sufficiently accurate.

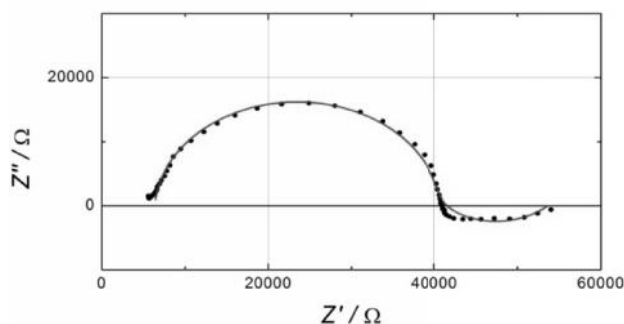


Fig. 10. Nyquist plot of experimental (points) and simulated (solid line) data for HER at -1.5 V and partially polished Zr in borate buffer. Simulation used the following values of Chart 1 circuit: R1=13kΩ , R2=6.4kΩ , R3=34kΩ, CPE1T=23.4 nF, CPE1P=0.96 , CPE2T=-3.53 μF , CPE2P=1.5.

We suppose to explore low frequency features in the future examining their dependence on time, deposition potential and pH of the medium.

CONCLUSIONS

Zirconium microelectrode in a form of a disc fitted in glass enables controllable polishing and reproducibility of the voltammetric and impedance data. Freshly polished electrode has to be inserted in the sample solution with an immediate application of a potential at which the oxidation of

Zr is prevented. The formation of ZrO₂ surface layer begins at -0.5 V. The hydrogen evolution reaction (HER) was investigated in the range of potentials -1.2 to -1.5 V and a single-electron transfer with transfer coefficient = 0.5 was confirmed. The presence of surface oxide layer effectively retards the HER and yields additional low frequency impedance loops attributed to the adsorption effects.

Acknowledgements: This research was supported by the Grant Agency of the Czech Republic (16-03085S).

REFERENCES

1. Z. Stoynov, D. Vladikova, D. Differential Impedance Analysis, Marin Drinov Publ. House, Sofia, 2005.
2. R. Causey, D. Cowgill, B. Nilson, Review of the Oxidation Rate of Zirconium Alloys. 2006, Report of Sandia National Lab., Livermore, CA, USA.
3. J.Chang, L.You-Sheng, L.; Karen, C. Rapid thermal chemical vapor deposition of zirconium oxide for metal-oxide-semiconductor field effect transistor application, *J. Vacuum Sci.. Technol. B*, **19**, 1782 (2001).
4. Y. Chen, M. Urquidi-Macdonald, D. Macdonald, The electrochemistry of zirconium in aqueous solutions at elevated temperatures and pressures, *J. Nucl. Mater.*, **348**, 133 (2006).
5. G. Nagy, Z. Kerner, G. Battistig, A. Pintér-Czordás, J. Balogh, T. Pajkossy, Oxide layers of Zr-1% Nb under PWR primary circuit conditions, *J. Nucl. Mater.*, **297**, 62 (2001).
6. G. Nagy, Z. Kerner, T. Pajkossy, In situ electrochemical impedance spectroscopy of Zr-1% Nb under VVER primary circuit conditions. *J. Nucl. Mater.*, **300**, 230 (2002).
7. J. Macák, R. Novotný, P. Sajdl, V. Ren iuková, V. Vrtílková, Electrochemical study of pre- and post-transition corrosion of Zr alloys in PWR coolant, Proc. of 15th Int. Conf. on Environmental Degradation of Materials in Nuclear Power Systems – Water Reactors, Wiley Inc., 621 (2011).
8. A. Krausová, J. Macák, P. Sajdl, R. Novotný, V. Ren iuková, V. Vrtílková, In-situ electrochemical study of Zr-Nb alloy corrosion in high temperature Li⁺ containing water. *J. Nucl. Mater.*, **467**, 302 (2015).
9. A. Krausová, J. Macák, P. Sajdl, V. Ren iuková, R. Novotný, Corrosion of Zr-Nb and Zr-Sn alloys under simulated condition of VVER reactor. *Corrosion and Material Protection* (in Czech), **59**, 99 (2015).
10. A. Lasia, *Electrochemical Impedance Spectroscopy and its Applications*. Springer, New York, 2014, Chapter 5.
11. A. Frumkin in: P. Delahay (Ed.), *Advances in Electrochemistry and Electrochemical Engineering*, vol. 3, Interscience, New York, 1963.
12. C. Montella, EIS study of hydrogen insertion under restricted diffusion conditions. I. Two-step insertion reaction. *J. Electroanal. Chem.*, **497**, 3 (2001).
13. E. Castro, M. de Giz, E. Gonzalez, J. Vilche, *Electrochim. Acta*, **42**, 951 (1997).

1* , 2 , 1
2 1 - ” “ 3 ,
I ,
30 2016 . ; 29 2016 .
()
(Zr)
0.5 V (Ag|AgCl|1M-LiCl)
ZrO₂.